Fast 2-D Direction of Arrival Estimation using Two-Stage Gridless Compressive Sensing

Mert Kalfa
ASELSAN Research Center
ASELSAN Inc.
Ankara, TR-06370, Turkey
Email: mkalfa@aselsan.com.tr

H. Emre Güven
ASELSAN Research Center
ASELSAN Inc.
Ankara, TR-06370, Turkey

***Abstract*—In this study, we propose and demonstrate a two-dimensional direction of arrival estimation method based on gridless compressive sensing (CS). The method is based on a gridless covariance fitting technique to alleviate the well-known grid mismatch problem of compressive sensing. Classical methods of gridless compressive sensing are limited to 1-D arrays, while extensions to multidimensional arrays are computationally demanding. To overcome these limitations, we introduce a two-stage solution with an angle-pairing matching pursuit algorithm, which enables 2-D arrays with lower computational complexity. We validate the method via numerical experiments on a cross-shaped generic array, then we compare the results with those of widely used methods such as MUSIC and beamforming.**

I. Introduction

Direction of arrival (DoA) estimation is a critical component for radar, electronic defense, and signal intelligence applications, where the spatial diversity introduced by a sensor array can be used to estimate the directions of targets. The simplest and most common technique is the beamforming method, where the spectral domain counterpart of the received signal over the spatial domain is used to estimate the target direction. However, classical beamforming suffers from low resolution, especially for correlated sources.

When there are multiple 'snapshots' of the scene, which is typical for most applications, covariance-based methods such as the Capon's Beamformer [1], Multiple Signal Classification (MUSIC) [2], Estimation of Parameters by Rotational Invariant Techniques (ESPRIT) [3], and their variants are widely used in modern systems. Although covariance-based algorithms enhance resolution, they also usually require a good estimate of the data covariance matrix, which in turn requires more snapshots. In practice, sufficient number of snapshots may not always be available, especially for fast changing scenes or sensors on moving platforms.

Recently, with the introduction of Compressive Sensing (CS) techniques and their corresponding recovery guarantees [4]–[6] a whole new set of tools have been made available for the DoA estimation problem. The main attraction of CS is that it allows the unique solution of an underdetermined and noisy linear system of equations in the form $\mathbf{y} = \mathbf{A}\mathbf{x} + \mathbf{n}$, which enables data reduction (in the case of DoA, reduction of number of sensor elements [7]) without compromising the performance.

In the so-called on-grid methods, the target directions can be recovered by using a pre-defined set of steering vectors and an l_1-norm minimization technique such as LASSO [8], or a maximum likelihood estimation (MLE) technique such as SPICE [9]. However, in reality the actual targets are never exactly on a pre-defined grid. The resulting grid mismatch problem is much more significant in CS compared to classical methods, since the reconstruction is non-linear and the solution to grid mismatch is not straightforward [10]–[13]. Moreover, using a denser grid to reduce the grid mismatch makes the neighbouring steering vectors more coherent, which in turn weakens the restrictive isometry property (RIP) [14] required for reconstruction guarantees.

There are two main classes of methods to tackle the off-grid problem. The first class is called the off-grid sparse methods where a either a fixed or dynamic grid is defined and the reconstruction involves estimating the target direction on the grid as well as the deviation from the grid [15]–[19]. These methods still require either a pre-defined grid or the number of grid elements (i.e., number of *atoms*), whose selection highly affects the performance. The second class is called *gridless* methods that operate over the continuous domain and hence require no gridding of the scene. The gridless methods exploit the Toeplitz structure of the data covariance matrix [20], which can be estimated via deterministic optimization methods such as Atomic Norm Minimization (ANM) [21]–[23] and Hankel-based Nuclear Norm Minimiziaton [24] or via covariance fitting methods such as Gridless SPICE (GLS) [25]. An important restriction of the Toeplitz structure imposed by the gridless methods is that the sensor must either be a 1-D uniform linear array (ULA) or a sparse linear array (SLA) subsampled from a 1-D ULA.

Previous work on extending the gridless formulations to 2-D arrays includes exploiting two-level Toeplitz structures [26], [27], and joint optimization for two orthogonal dimensions [28], [29]. However, both classes of methods result in a semidefinite programming (SDP) problem with number of constraints in $O(N_x N_y)$, where N_x and N_y are the number of lattice points for the array along x and y axes, respectively. The SDP becomes infeasible when the number of sensor elements are much smaller than the number of available grid points, e.g., sparse arrays or a cross-shaped array that is widely used for DoA applications.

In this work, we propose a fast two-stage direction-of-arrival estimation method for use on 2-D cross-shaped sparse arrays. The proposed method operates over a continuous domain and hence does not suffer from the grid mismatch problem, while remaining applicable to 2-D arrays. Moreover, thanks to its two-stage decoupled formulation, the number of SDP constraints is in $O(\max\{N_x, N_y\})$, which makes it much faster than existing 2-D gridless methods.

The rest of this paper is organized as follows. Section II presents the data model. Section III describes the proposed method in detail. Section IV presents the numerical results. Concluding remarks are given in Section V.

II. Signal Model

We consider the cross-shaped planar array geometry shown in Fig. 1. The array consists of two orthogonal 1-D ULAs or SLAs, possibly with a shared element. There are K uncorrelated, narrowband and far-field sources impinging on the array that are sampled L consecutive times, (i.e., L is the number of snapshots). The received signals in the 1-D arrays along x and y axes are given by

$$\mathbf{X} = \mathbf{A_x}\mathbf{S} + \mathbf{V_x}, \tag{1}$$

$$\mathbf{Y} = \mathbf{A_y}\mathbf{S} + \mathbf{V_y}, \tag{2}$$

where $\mathbf{X} \in \mathbb{C}^{N_x \times L}$ and $\mathbf{Y} \in \mathbb{C}^{N_y \times L}$ are the measured vectors with L snapshots, $\mathbf{V_x} \in \mathbb{C}^{N_x \times L}$ and $\mathbf{N_y} \in \mathbb{C}^{N_y \times L}$ are the noise matrices whose entries are i.i.d. complex Gaussian with a mean of zero and variance σ_0^2. In (1), $\mathbf{S} \in \mathbb{C}^{K \times L}$ is the matrix consisting of the source amplitudes across each snapshot, and $\mathbf{A_x} \in \mathbb{C}^{N_x \times K}$ is the steering matrix (i.e., the manifold) for the array along x axis, defined as

$$\mathbf{A_x} = \left[\mathbf{a_x}\left(f_{x_1}\right), \ldots, \mathbf{a_x}\left(f_{x_K}\right)\right], \tag{3}$$

where

$$\mathbf{a_x}\left(f_{x_k}\right) = \left[1, e^{-j2\pi f_{x_k}}, \ldots, e^{-j2\pi(M_x-1)f_{x_k}}\right]^{\mathrm{T}}, \tag{4}$$

$$f_{x_k} = (d/\lambda)\sin(\theta_k)\cos(\phi_k), \tag{5}$$

and similarly for $\mathbf{A_y} \in \mathbb{C}^{N_y \times K}$

$$\mathbf{a_y}\left(f_{y_k}\right) = \left[1, e^{-j2\pi f_{y_k}}, \ldots, e^{-j2\pi(M_y-1)f_{y_k}}\right]^{\mathrm{T}}, \tag{6}$$

$$f_{y_k} = (d/\lambda)\sin(\theta_k)\sin(\phi_k), \tag{7}$$

where T is the matrix transpose, λ is the free-space wavelength at the operating frequency and d is the inter-element spacing.

For SLAs, we select a subset of the rows of $\mathbf{X}$ and $\mathbf{Y}$, which we define as $\mathbf{X}_{\mathbf{\Omega_x}} = \mathbf{\Gamma_x}\mathbf{X}$ and $\mathbf{Y}_{\mathbf{\Omega_y}} = \mathbf{\Gamma_y}\mathbf{Y}$, where $\mathbf{\Gamma_x} \in \{0,1\}^{M_x \times N_x}$ and $\mathbf{\Gamma_y} \in \{0,1\}^{M_y \times N_y}$ are the row selection matrices for the *virtual* ULAs along x and y axes, respectively.

III. Proposed Method

The proposed method is based on the Gridless SPICE (GLS) [25]. For a 1-D SLA with a selection matrix of $\mathbf{\Gamma}$ when the number of snapshots is larger than the number of elements

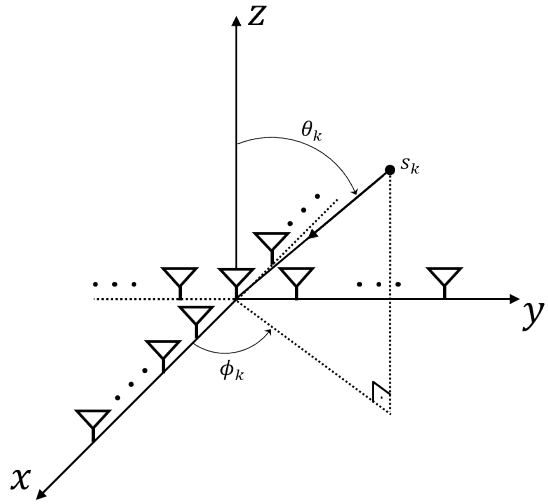

Fig. 1. Direction of arrival estimation problem geometry.

(i.e., $L \geq M$), the covariance fitting of the GLS can be cast as the following semidefinite programming (SDP) problem

$$\begin{aligned} &\underset{\mathbf{Z},\mathbf{u}}{\arg\min} \left\{ \mathrm{Tr}(\mathbf{Z}) + \mathrm{Tr}\left(\mathbf{\Gamma}^{\mathrm{T}}\tilde{\mathbf{R}}^{-1}\mathbf{\Gamma}\,\mathbf{T}(\mathbf{u})\right) \right\}, \\ &\qquad \text{subject to} \begin{bmatrix} \mathbf{Z} & \tilde{\mathbf{R}}^{\frac{1}{2}} \\ \tilde{\mathbf{R}}^{\frac{1}{2}} & \mathbf{\Gamma}\,\mathbf{T}(\mathbf{u})\mathbf{\Gamma}^{\mathrm{T}} \end{bmatrix} \geq \mathbf{0}, \end{aligned} \tag{8}$$

where $\mathrm{Tr}(.)$ is the trace operator, $\tilde{\mathbf{R}} = \frac{1}{L}\mathbf{X}\mathbf{X}^{\mathrm{H}}$ is the sample covariance, $\mathbf{Z}$ is a free variable, $\geq \mathbf{0}$ denotes nonnegative definiteness, and $\mathbf{T}(\mathbf{u}) \in \mathbb{C}^{NxN}$ is a Hermitian Toeplitz matrix whose first row is the vector $\mathbf{u}^{\mathrm{T}}$. Note that $\mathbf{T}(\mathbf{u})$ corresponds to the noisy data covariance matrix for the full ULA case.

When $L < M$, the sample covariance matrix is singular; thus, the modified covariance fitting problem is given by

$$\begin{aligned} &\underset{\mathbf{Z},\mathbf{u}}{\arg\min} \left\{ \mathrm{Tr}(\mathbf{Z}) + \mathrm{Tr}\left(\mathbf{\Gamma}^{\mathrm{T}}\mathbf{\Gamma}\,\mathbf{T}(\mathbf{u})\right) \right\}, \\ &\qquad \text{subject to} \begin{bmatrix} \mathbf{Z} & \tilde{\mathbf{R}} \\ \tilde{\mathbf{R}} & \mathbf{\Gamma}\,\mathbf{T}(\mathbf{u})\mathbf{\Gamma}^{\mathrm{T}} \end{bmatrix} \geq \mathbf{0}. \end{aligned} \tag{9}$$

After finding $\mathbf{T}(\mathbf{u})$ from (8) or (9), the embedded frequencies (corresponding to DoAs) can be recovered uniquely from the Vandermonde decomposition of the Toeplitz matrices given by

$$\mathbf{T}(\mathbf{u}) = \mathbf{A}(\mathbf{f})\,\mathrm{diag}(\mathbf{p})\mathbf{A}^{\mathrm{H}}(\mathbf{f}) + \sigma_0^2\mathbf{I}. \tag{10}$$

Equation (10) can be solved by the generalized pencil of function (GPOF) method [30], which is less noise sensitive compared to the widely used Prony's method [31]. During this stage, the number of sources is estimated using the SORTE algorithm [32], which is shown to be robust under noise especially for sparse recovery problems.

In the proposed method, we use GLS sequentially on two orthogonal 1-D arrays as shown in Fig. 1. As a result, we obtain two sets of spatial frequencies ($\mathbf{f}_x$ and $\mathbf{f}_y$). To correctly pair the two sets and resolve the ambiguity, we use a matching pursuit algorithm based on beamforming. First, the sample covariance of the whole array is calculated as

$$\tilde{\mathbf{R}}_{2D} = \begin{bmatrix} \mathbf{X} \\ \mathbf{Y} \end{bmatrix} \begin{bmatrix} \mathbf{X}^{\mathrm{H}} & \mathbf{Y}^{\mathrm{H}} \end{bmatrix} \tag{11}$$

Then, the array manifold for each of the frequency pairs ($f_{x_i} \in \mathbf{f}_x$ and $f_{y_j} \in \mathbf{f}_y$) is calculated as

$$\mathbf{A}_{2D}(\mathbf{f}_x, \mathbf{f}_y) = \left[e^{-j2\pi \left(x_m f_{x_i} + y_m f_{y_j} \right)/\lambda} \right] \in \mathbb{C}^{M \times K^2}, \tag{12}$$

where x_m and y_m with $m = 1, \ldots, M$ are the coordinates of the m^{th} element in the array. The proposed pairing algorithm iteratively finds the most likely candidate among all possible pairs, then calculates the residue of the data covariance matrix when the effect of most likely pair is eliminated. We repeat this procedure until we reach the desired number of pairs (K). The overall procedure, which we call GLS^2, is summarized in Algorithm 1.

Algorithm 1: *GLS^2: Two-stage Gridless SPICE*

1. Solve for $\mathbf{T}_x(\mathbf{u})$ using (8) or (9)
2. Solve for $\mathbf{T}_y(\mathbf{u})$ using (8) or (9)
3. Estimate the number of sources (K) using SORTE [32]
4. Find $\mathbf{f}_x = f_{x_1}, \ldots, f_{x_K}$ from $\mathbf{T}_x(\mathbf{u})$ using GPOF [30]
5. Find $\mathbf{f}_y = f_{y_1}, \ldots, f_{y_K}$ from $\mathbf{T}_y(\mathbf{u})$ using GPOF [30]
6. Construct the full sample covariance matrix $\tilde{R}_{2D}$ in (11)
7. Construct 2-D array manifold $\mathbf{A}_{2D}$ in (12)
8. Set $\mathbf{F_{xy}} = \{\emptyset\}$, $\mathbf{R} = \tilde{\mathbf{R}}_{2D}$
9. **for** $i = 1, \ldots, K$
10. $p = \max \left(\mathrm{diag} \left(\mathbf{A}_{2D}^{\mathrm{H}} \; \mathbf{R} \; \mathbf{A}_{2D} \right) \right)$
11. $(f_x, f_y) = \arg\max_{(f_x, f_y)} \left(\mathrm{diag} \left(\mathbf{A}_{2D}^{\mathrm{H}} \; \mathbf{R} \; \mathbf{A}_{2D} \right) \right)$
12. $\mathbf{R} = \mathbf{R} - \left(p/(M_x + M_y)^2 \right) \mathbf{A}_{2D}(f_x, f_y) \; \mathbf{A}_{2D}^{\mathrm{H}}(f_x, f_y)$
13. $\mathbf{F_{xy}} = (\mathbf{F_{xy}}; \; (f_x, f_y))$
14. **endfor**
15. Convert $\mathbf{F_{xy}}$ to spherical angles using (5) and (7)

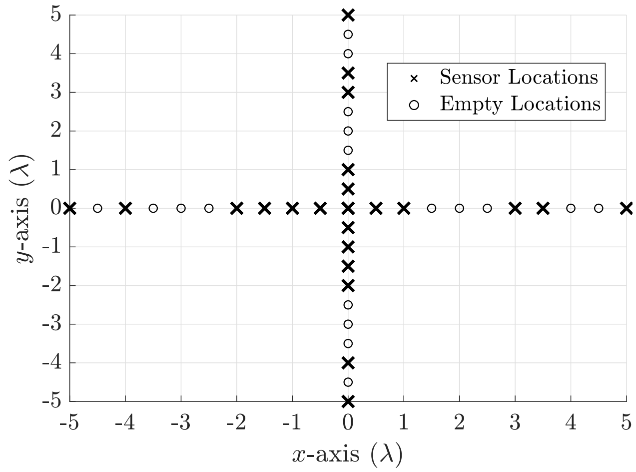

Fig. 2. Selected Array Geometry.

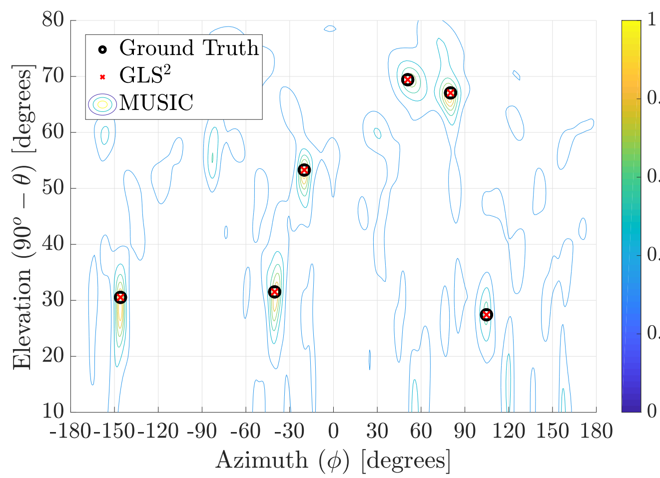

Fig. 3. GLS^2 vs. MUSIC for $K = 6$, SNR $= 0$ dB, and $L = 20$.

IV. Numerical Results

To demonstrate the validity of the proposed method, a generic array lattice is selected with $N_x = N_y = 21$, $M_x = M_y = 12$, $d = \lambda/2$, and

$$\Omega_x = \Omega_y = \{1, 3, 7, 8, 9, 10, 11, 12, 13, 17, 18, 21\}. \tag{13}$$

Note that the center element in both linear arrays are shared. The resulting 23-element array from (13) is illustrated in Fig. 2.

In our simulations, there are $K = 6$ narrowband, far-field, and uncorrelated sources impinging on the array. The source locations are chosen arbitrarily from the upper hemisphere as

$$\begin{aligned} \{(\phi_k, \theta_k)\} = \{&(-145.9^o, 59.5^o), (-40.3^o, 58.5^o), \\ &(-20^o, 36.7^o), (50.9^o, 20.6^o), \\ &(80.2^o, 22.9^o), (104.8^o, 62.6^o)\}, \end{aligned} \tag{14}$$

while the source amplitudes $\mathbf{S}$ are chosen such that their magnitude is unity while their phases are independently and uniformly distributed in $[0, 2\pi)$ for each snapshot. With the given parameters above, the DoA estimation problem is solved via the proposed method (GLS^2), beamforming, and MUSIC. Note that GLS^2 does not require advance knowledge of the noise variance and the number of sources, while beamforming and MUSIC require the number of sources for correct localization. Also note that GLS^2 is a decoupled algorithm, i.e., it utilizes half of the array at a given time. Therefore GLS^2 has approximately 3 dB lower array processing gain than any method that utilizes the whole array at once. However, the results show that GLS^2 outperforms the conventional methods despite this disadvantage

Figure 3 shows the normalized outputs of GLS^2 and MUSIC for a single case with SNR$=$ 0 dB, and $L = 20$. Note that DoAs are given in terms of azimuth ($AZ = \phi$) and elevation ($EL = 90^o - \theta$). Also, we do not include beamforming in Fig. 3 for clarity. Thanks to SORTE and GPOF algorithms used in steps 3–5 of Algorithm 1, the only outputs of GLS^2 are the DoAs and the corresponding signal powers (not shown in Fig. 3).

To better illustrate the localization performance of GLS^2, we performed a Monte Carlo simulation with 1000 iterations for various SNR levels. Figure 4 shows DoA estimation results for the whole Monte Carlo run for GLS^2, beamforming, and MUSIC as scatter graphs at SNR $= 0$ dB and $L = 100$. Note that the uncertainty along elevation is significantly more than

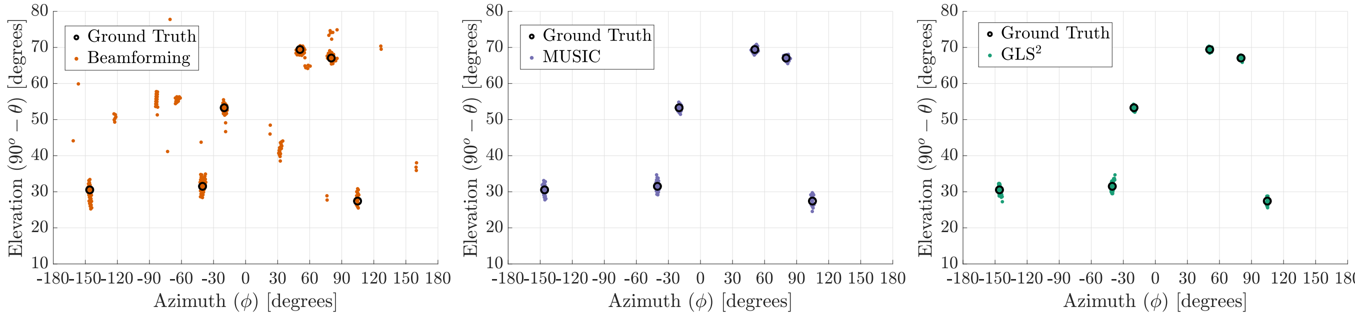

(a) (b) (c)

Fig. 4. DoA Estimation Results over 1000 Monte Carlo simulations with $K = 6$, SNR = 0 dB, $L = 100$ (a) Beamforming (b) MUSIC (c) GLS^2

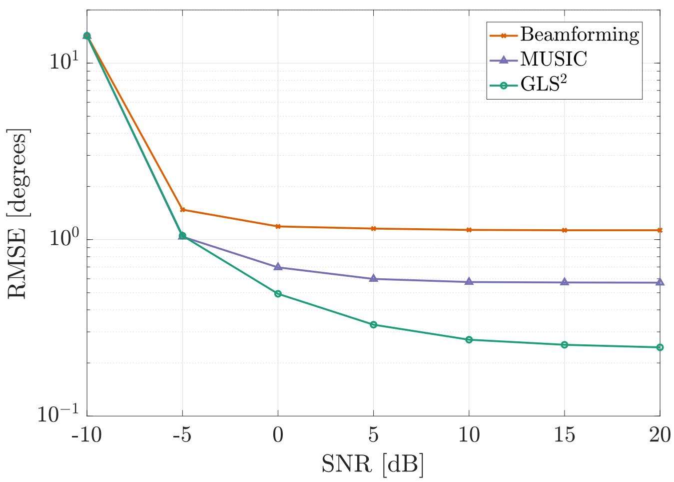

Fig. 5. RMSE Comparison when $K = 6$ and $L = 400$.

the uncertainty along azimuth (also visible in Fig. 3). This is due to the array being placed in the xy-plane, which makes the projected size of the array aperture vary little across azimuth angles, while the projections along elevation angles scales with $\sin(EL)$. This effect can also be observed from the decreasing uncertainty as the elevation angle gets larger in Fig. 4.

Finally, to demonstrate the robustness of GLS^2 over varying SNR levels, the root mean square error (RMSE) of the estimated DoA angles is defined as

$$RMSE = \sqrt{\sum_{n=1}^{N_{MC}} \left(\|\hat{\theta} - \theta\|_2^2 + \|\hat{\phi} - \phi\|_2^2\right) / (KN_{MC})}, \tag{15}$$

where N_{MC} is the number of Monte Carlo iterations (i.e., trials). The RMSE for GLS^2 is calculated for $N_{MC} = 1000$ and compared to the RMSEs of beamforming and MUSIC in Fig. 5 for $L = 400$. Figure 5 clearly shows that GLS^2 performs much better than beamforming across a wide range of SNR levels, and is significantly better than MUSIC in high-SNR regimes. Even in low-SNR regimes, the proposed method performs as well as MUSIC. It is noteworthy that GLS^2 provides improved performance despite the lower array processing gain due to utilizing each orthogonal half of the array sequentially.

V. Conclusion

In this work, we introduced and demonstrated a fast two-stage gridless compressive sensing method for 2-D DoA estimation. The proposed method overcomes the limitation of gridless sparse DoA estimation methods to uniform 1-D arrays, while providing a fast alternative to the computationally costly 2-D methods available in the literature. The proposed GLS^2 method outperforms conventional DoA estimation methods such as beamforming and MUSIC, despite its disadvantage in terms of array processing gain. The future work on the subject includes extending the method to utilize the entire array coherently at a reasonable computational efficiency, and incorporating arbitrary array geometries.

Acknowledgment

The authors thank Prof. Orhan Arıkan for many hours of fruitful discussions.

References

[1] J. Capon, “High resolution frequency-wavenumber spectrum analysis,” *Proc. IEEE*, vol. 57, pp. 1408–1418, Aug. 1969.

[2] R. Schmidt, “Multiple emitter location and signal parameter estimation,” *IEEE Trans. Antennas Propagat.*, vol. 34, no. 3, pp. 276–280, Mar. 1986.

[3] R. Roy, T. Kailath, “ESPRIT–estimation of signal parameters via rotational invariance techniques,” *IEEE Trans. Acoust., Speech, Signal Process.*, vol. 37, no. 7, Jul. 1989.

[4] D. Donoho, “Compressed sensing,” *IEEE Trans. Inform. Theory*, vol. 52, no. 4, pp. 1289–1306, 2006.

[5] E. Candes, J. Romberg, T. Tao, “Robust uncertainty principles: exact signal reconstruction from highly incomplete frequency information,” *IEEE Trans. Inform. Theory*, vol. 52, pp. 489–509, 2006.

[6] R. Baraniuk, “Compressive sensing,” *IEEE Signal. Process. Mag.*, vol. 24, no. 4, pp. 118–121, Jul. 2007.

[7] X. Wang, E. Aboutanios, M. G. Amin, “Adaptive array thinning for enhanced DOA estimation,” *IEEE Signal Process. Lett.*, vol. 22, no. 7, pp. 799–803, 2006.

[8] R. Tibshirani, “Regression shrinkage and selection via the LASSO,” *Journal of the Royal Statistical Society*, vol. 58, no. 1, pp. 267–288, 1996.

[9] P. Stoica, P. Babu, J. Li, “SPICE: a sparse covariance-based estimation method for array processing,” *IEEE Trans. Signal Process.*, vol. 59, no. 2, pp. 629–638, Feb. 2011.

[10] Y. Chi, L. Scharf, A. Pezeshki, R. Calderbank, “The sensitivity to basis mismatch of compressed sensing in spectrum analysis and beamforming,” *6th Workshop on Defense Applications of Signal Processing (DASP)*, Lihue, October, 2009.

[11] M. Herman, T. Strohmer, "General deviants: an analysis of perturbations in compressed sensing," *IEEE J. Sel. Top. Signal Process.*, vol. 4, no. 2, pp. 342–349, 2010.

[12] Y. Chi, L. Scharf, A. Pezeshki, R. Calderbank, "Sensitivity of basis mismatch to compressed sensing," *IEEE Trans. Signal Process.*, vol. 59, pp. 2182-2195, 2011.

[13] D.H. Chae, P. Sadeghi, R. Kennedy, "Effects of basis-mismatch in compressive sampling of continuous sinusoidal signals," *International Conference on Future Computer and Communication (ICFCC)*, pp. 739-743, 2010.

[14] R. Baraniuk, M. Davenport, R. DeVore, M. Wakin, "A simple proof of the restricted isometry property for random matrices," *Constructive Approximation*, vol. 28, no. 3, pp. 253–263, Dec. 2008.

[15] Z. Yang, C. Zhang, L. Xie, "Robustly stable signal recovery in compressed sensing with structured matrix perturbation," *IEEE Trans. Signal Process.*, vol. 60, no. 9, pp. 4658–4671, 2012.

[16] Z. Yang, L. Xie, C. Zhang, "Off-grid direction of arrival estimation using sparse Bayesian inference," *IEEE Trans. Signal Process.*, vol. 61, no. 1, pp. 38–43, 2013.

[17] X. Wu, W.-P. Zhu, J. Yan, "Direction of arrival estimation for off-grid signals based on sparse Bayesian learning," *IEEE Sensors J.*, vol. 16, no. 7, pp. 2004–2016, 2016.

[18] S. Bernhardt, R. Boyer, S. Marcos, P. Larzabal, "Compressed sensing with basis mismatch: performance bounds and sparse-based estimator," *IEEE Trans. Signal Process.*, vol. 64, no. 13, pp. 3483–3494, 2016.

[19] O. Teke, A. C. Gurbuz, O. Arikan, "A robust compressive sensing based technique for reconstruction of sparse radar scenes," *Digital Signal Processing*, vol. 27, pp. 23–32, 2014.

[20] V.F. Pisarenko, "The retrieval of harmonics from a covariance function," *Geophysical Journal International*, vol. 33, no. 3, pp. 347–366, 1973.

[21] V. Chandrasekaran, B. Recht, P. A. Parrilo, A. S. Willsky, "The convex geometry of linear inverse problems," *Foundations of Computational Mathematics*, vol. 12, no. 6, pp. 805–849, 2012.

[22] B. N. Bhaskar, G. Tang, B. Recht, "Atomic norm denoising with applications to line spectral estimation," *IEEE Trans. Signal Process.*, vol. 61, no. 23, pp. 5987-5999, 2013.

[23] Z. Yang, L. Xie, "Enhancing sparsity and resolution via reweighted atomic norm minimization," *IEEE Trans. Signal Process.*, vol. 64, no. 4, pp. 995–1006, Feb. 2016.

[24] Y. Chen, Y. Chi, "Robust spectral compressed sensing via structured matrix completion," *IEEE Trans. Inform. Theory*, vol. 60, no. 10, pp. 6576–6601, 2014.

[25] Z. Yang, L. Xie, "On gridless sparse methods for line spectral estimation from complete and incomplete data," *IEEE Trans. Signal Process.*, vol. 63, no. 12, pp. 3139–3153, Jun. 2015.

[26] Y. Chi, Y. Chen, "Compressive two-dimensional harmonic retrieval via atomic norm minimization," *IEEE Trans. Signal Process.*, vol. 63, no. 4, pp. 1030–1042, 2015.

[27] Z. Yang, L. Xie, P. Stoica, "Vandermonde decomposition of multi-level Toeplitz matrices with application to multidimensional super-resolution," *IEEE Trans. Inform. Theory*, vol. 62, no. 6, pp. 3685–3701, 2016.

[28] L. Xiang, Q. Huang, L. Zhang, K. Liu, "Joint 2-D DOA estimation using gridless sparse method," *2016 IEEE 13th International Conference on Signal Processing (ICSP)*, pp. 434–437, Chengdu, 2016.

[29] X. Wu, W. P. Zhu, J. Yan,"A fast gridless covariance matrix reconstruction method for one- and two-dimensional direction-of-arrival estimation," *IEEE Sensors J.*, vol. 17, no. 15, pp. 4916–4927, Aug. 2017.

[30] Y. Hua, T. Sarkar, "Generalized pencil-of-function method for extracting poles of an EM system from its transient response," *IEEE Trans. Antennas Propagat.*, vol. 37, no. 2, pp. 229–234, 1989.

[31] M. L. V. Blaricum, R. Mittra, "Problem and solutions associated with Prony's method for processing transient data," *IEEE Trans. Antennas Propagat.*, vol. AP-26, pp. 174–182, 1978.

[32] Z. He, A. Cichocki, S. Xie and K. Choi, "Detecting the number of clusters in n-way probabilistic clustering," *IEEE Trans. Pattern Anal. Mach. Intell.*, vol. 32, no. 11, pp. 2006–2021, Nov. 2010.